Response to Anonymous Referee #2 (Major comments)

We would like to thank Anonymous Referee #2 for his / her critical comments helping us to improve our paper.

Major issue 1 (error analysis)

We carried out an error analysis and will present the results in a new chapter (*4.3.3 Basic error analysis*) as follows:

"For heights of cloud tops considered as true positives in the visual validation a simple error analysis was carried out. Three main error sources were identified:

1. Misfits between the reprojected DEM and the real landscape as seen from the main cam. They are caused by an imperfect automatic adjustment of the virtual camera (cf. Sect. 4.2.1) as well as small image distortions (cf. Sect. 4.1). To quantify the size of this error 20 randomly chosen scenes with a correctly detected cloud top appearance and a visible horizon were analyzed. For each scene the deviation in pixels between the position of a mountain top (in a distance of ~15300 m to the main cam, cf. Fig. 4 [a marker will be added to Fig. 4]) in the mean image and in the reprojected DEM was calculated. The RMSD calculated from these deviations ($RMSD_1$) is 2.73 pixels. These 2.73 pixels correspond to a height difference of

$$\Delta h = 2.73\ px * (|d| * \cos(\gamma) / 1333\ px) * (1/\cos(\beta-90°)) * \sin(\alpha) \qquad \text{(eq. x)}$$

with |d| being the length of the vector $\vec{d}$ from the camera to the observed cloud top and γ being the angle between the camera's viewing direction and $\vec{d}$. β is the angle between $\vec{d}$ and the slope on which the cloud heights are measured. α is the steepness of the terrain measured as an angle (cf. Fig. xx).

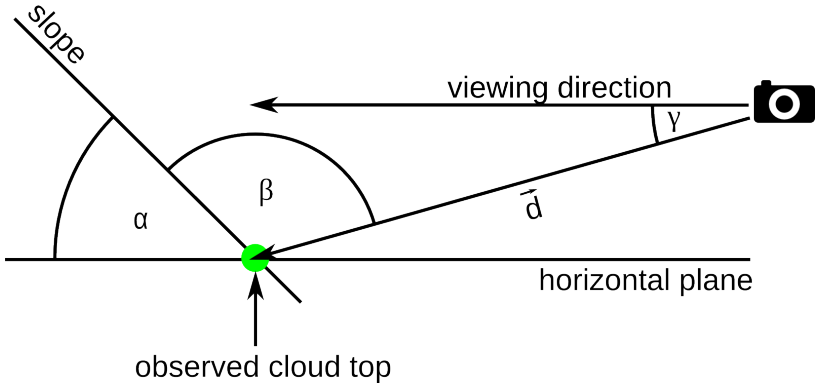

Fig. xx: Definitions used in Eq. x

2. Blurriness of the cloud tops. In Sect. 4.3.1 cloud tops were considered as true positives if they had been correctly detected at the transition between cloud and non-cloud areas. This transition, however, is not a distinct edge in all cases and may extend over altitude differences of several meters. The 'real' cloud top height - for instance defined as the height in which the the World Meteorological Organization's definition of fog (cf. Sect. 1) is fulfilled - is located somewhere in this transition zone. For 20 randomly chosen scenes with a correctly detected cloud top appearance these transitions zones were visually identified in the two-dimensional mean image

and their height was calculated using the reprojected DEM. It was assumed that the deviation between real cloud top heights as well as the detected cloud top heights would be typically half the height of the transition zone. The RMSD calculated from these deviations ($RMSD_2$) is 41.93 m.

3. Imprecisions of the ASTER GDEM 2. The RMSD for the ASTER GDEM 2 ($RMSD_3$) calculated using GPS measurements is given as 8.68 m by Tachikawa et al. (2011). [This information will also be added to chapter 3 where the 95% confidence interval of the DEM is given]

If for each of these error sources the RMSD is assumed to be the typical uncertainty caused by it, according to the Gaussian law of error propagation for additive magnitudes the uncertainty u_H of the retrieved cloud top heights can be calculated as

$$u_H = \sqrt{RMSD_1^2 + RMSD_2^2 + RMSD_3^2} = \sqrt{(2.73\,px * (|d| * \cos(\gamma)/1333\,px) * (1/\cos(\beta - 90°)) * \sin(\alpha))^2 + 1833.47} \quad \text{(eq. xx)}$$

For a vertical slope, directly facing orthogonally towards the viewing direction of the camera in a distance of 2500 m and the camera being orientated horizontally this would result in $u_H = 43.12\,m$."

Additionally p. 2805, l. 6-8 will be changed as follows:
"The detection of cloud top positions in the 2D image as well as the projection onto the three-dimensional DEM work well for the camera location in the Taroko Gorge, **although the derived heights are afflicted with uncertainties of above 40 m that are mostly caused by the blurriness of cloud tops (cf. Sect. 4.3.3)**."

Major issue 2 (limitations of the method)

The algorithm has been partially validated during springtime in a snow-free valley. Is the technique limited to snow-free mountains?

We've addressed that issue in the minor comments as follows:

=> Even in winter snow is rare in Taiwan and limited to the highest peaks. Every pixel used for zCT determination in the Taroko Gorge is below an altitude of 3000 m, so that won't be a problem. For the adaptation of the method to other locations, however, this might be a problem. We will address that issue in the final paper as follows:

p. 2798, l. 2 – 3: "Since clouds are overall brighter than non cloud **(nor snow)** covered terrain (if analyzed for each fine segment separately) [...]"

p. 2805, l. 9 - 11 "Since a valid cloud height determination depends on clouds touching the terrain, the approach does only work for selected locations, ideally with frequently occurring sea of cloud conditions. **Also the occurrence of snow, which is unlikely for the area used for zCT determination in this study, might cause problems as the presented method relies on differences in the brightness between clouds and terrain.**"

In lack of footage from another location we can't say anymore on this issue.

Matthews correlation coefficient & different lighting conditions:

The manual as well as the automatic validation were redone incorporating the Matthews correlation coefficient and as well as a differentiation between lighting conditions ("affected by cloud shadows of overlying cloud layers" & "low sun"). Since the different classes would get too small otherwise the number of scenes incorporated in the visual validation was doubled to 20 % of all scenes.

The following changes in the text will be made:

p. 2800, l. 3 – 10: . "For ~~each of~~ these scenes the cloud top positions were calculated and validated using two different approaches. This was done by summarizing the validation results in **three** confusion matri**ces** for each validation approach. **One of these matrices contains all incorporated scenes. Another matrix contains scenes only that were taken under complex lighting conditions defined by a sun elevation between 5° and 15° (calculated using code from FMet (Cermak et al., 2008) additionally taking into account atmospheric refractions as described by Sæmundsson (1986)). Below a sun elevation of 5° the valley is located in the shadows of the surrounding mountains, which would result in an indirect illumination that could not be considered as a complex lighting condition. A third matrix contains scenes only in which the detection area was visibly affected by shadows of overlying broken cloud layers.** From these matrices the following statistical measures (Jollife and Stephenson, 2003; **Matthews, 1975**) were calculated (see Appendix A for formulas):

– proportion correct (PC)
– bias
– probability of detection (POD)
– probability of false detection (POFD)
– false alarm rate (FAR)
– Hanssen-Kuipers discriminant (HKD)
– Matthews correlation coefficient (MCC) [formula will be added to appendix]!

p. 2802, l. 18. will be changed to:
"~~10%~~ **20%** of the 8400 main cam scenes were randomly chosen and detected cloud top heights that were marked as shown in Fig. 8 were manually assessed."

Chapter 5.1 (Validation results) will be changed as follows:
"Tab. 1 shows the result of the validation based on the validation cam footage. The PC calculated from this matrix is **0.9498 (complex illumination: 0.9466, cloud shadow affected:0.9889)**. It is the only statistical measure described in Sect. 4.3 that can be interpreted in a meaningful way for the validation cam approach.

The results of the visual validation are shown in Tab. 2 and 3. These results show that the presence and absence as well as the height cloud tops in the two-dimensional camera footage was correctly determined in **84.73% (complex illumination: 83.23%, cloud shadow affected: 90.00%)** of the scenes (PC) while the frequency of

cloud tops in the area of detection was ~~slightly~~ underestimated in general **(bias: 0.8418, complex illumination: 0.8438, cloud shadow affected: 0.9927)** Cloud tops were detected in **77.21% (complex illumination: 78.13%, cloud shadow affected: 91.97%)** of the scenes in which cloud top were present (POD) and in **7.35 % (complex illumination: 9.23%, cloud shadow affected: 13.70%)** of the scenes were no cloud tops were present in the detection area **(POFD)**. This corresponds to about **8.28% (complex illumination: 7.41%, cloud shadow affected: 7.35%)** of the determined cloud tops being mistakenly detected (FAR)."

p. 2804, l. 18-20 (chapter 6: Discussion) will be changed as follows:

The results of the visual validation can be regarded as promising. The accuracy, the HKD and the POD are quite high and the PO**F**D and FAR are low. The Bias shows that the cloud frequency is only slightly underestimated. **The results for complex lighting conditions do only differ slightly from those for all scenes incorporated in the validation. The results for scenes affected by the shadows of overlying cloud layers are generally better (even if the POFD is slightly higher) than those for the other classes. This finding, however, might be strongly biased since the cloud shadow affected scenes are not randomly distributed over the investigation period but the appearance of cloud shadows is temporally clustered.**

p. 2805, l. 4-6 will be changed as follows:
The ability of the presented approach to determine the cloud top height for cases in which the presence of clouds is known was shown using the validation cam approach and can be regarded as good **for all scenes incorporated in the validation as well as for scenes under complex lighting conditions and for scenes that are affected by cloud shadows**.

p.2805, l. 15-17 will be changed as follows:
The adaptation to the footage of cameras below the cloud base that are used to derive zCB (cf. Sect. 4.2.4) could cause problems since cloud bases are ~~often~~ **generally more** blurry **than cloud tops**.

There seems to be a misunderstanding regarding p. 2804, l. 3-5:

"The algorithm also works for more complex lighting conditions (cf. Fig. 13) and – as long as the clouds are touching the terrain – in situations with a shattered cloud cover (cf. Fig. 14)."

With "shattered cloud cover" we were not referring to scenes affected by shadows caused by an OVERLYING shattered cloud cover but scenes were the sea of clouds itself is broken. We admit that these scenes are very rare so that a meaningful validation is not possible with our data. Also most of them are excluded from further analysis since they would not fulfil the sea-of-clouds-criterion (p. 2798, l. 20-27). Therefore this type of scenes is indeed not very relevant. We will change Fig. 14 to a scene affected by shadows of overlying clouds instead:

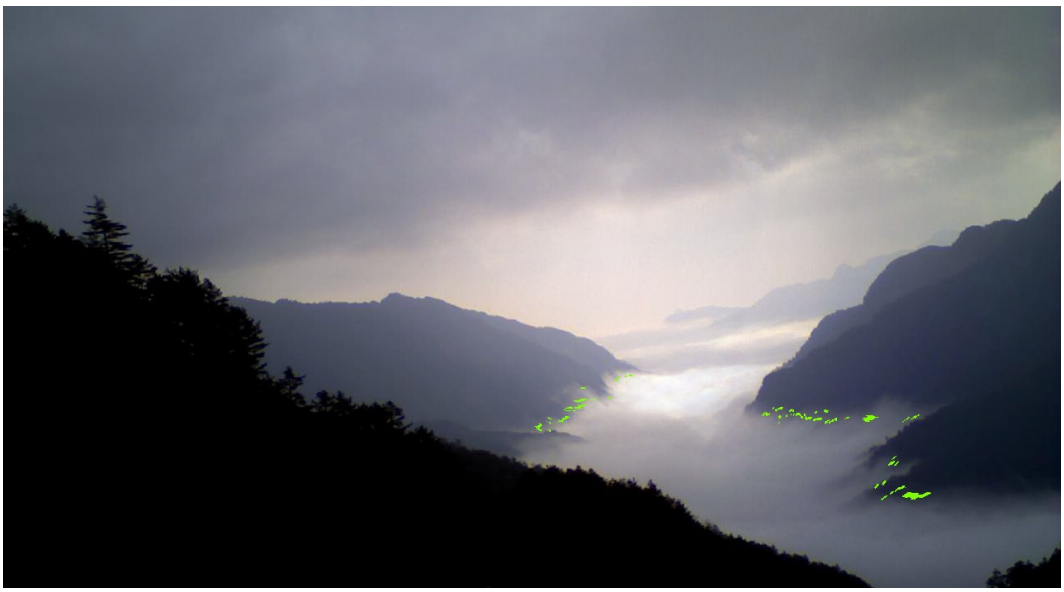

...and rephrase to:

"The algorithm also works for more complex lighting conditions (cf. Fig. 13) and ~~– as long as the clouds are touching the terrain – in situations with a shattered cloud cover~~ and for scenes affected by the shadows of overlying broken cloud layers.(cf. Fig. 14)."

"The algorithm also works for more complex lighting conditions (cf. Fig. 13) and for scenes affected by the shadows of overlying broken cloud layers. As long as the clouds are touching the terrain it also seems to work in situations with a shattered cloud cover instead a sea of clouds (cf. Fig. 14). While the latter can - due to a very small sample size of this class - only be assumed based on single scenes, the suitability of the method for scenes taken under complex lighting conditions and scenes affected by cloud shadows has been shown in the validation."

Tables 1, 2 & 3 will be changed as follows:

Table 1. Confusion matri**ces** for the automated validation. [The matrix has changed slightly for "all lighting conditions" since march 21st has accidentally not been incorporated in the analysis for the discussion paper]

Validation cam cloud immersed?	Validation cam below interpolated z_{CT}?		
	True / 1	False / 0	
True / 1	$n_{11} = 262$	$n_{10} = 9$	all lighting conditions
False / 0	$n_{01} = 49$	$n_{00} = 835$	
True / 1	$n_{11} = 41$	$n_{10} = 1$	complex illumination
False / 0	$n_{01} = 10$	$n_{00} = 154$	
True / 1	$n_{11} = 34$	$n_{10} = 2$	cloud shadow affected
False / 0	$n_{01} = 1$	$n_{00} = 144$	

Table 2. Confusion matrices for the visual validation.

Cloud tops present in detection area?	Cloud tops detected at correct position ?		
	True / 1	False / 0	
True / 1	$n_{11} = 454$	$n_{10} = 134$	all lighting conditions
False / 0	$n_{01} = 41$	$n_{00} = 517$	
True / 1	$n_{11} = 75$	$n_{10} = 21$	complex illumination
False / 0	$n_{01} = 6$	$n_{00} = 59$	
True / 1	$n_{11} = 126$	$n_{10} = 11$	cloud shadow affected
False / 0	$n_{01} = 10$	$n_{00} = 63$	

Table 3. Results of the visual validation.

PC	Bias	POD	POFD	FAR	HKD	MCC	
0.8473	0.8418	0.7721	0.0735	0.0828	0.6986	0.7050	all lighting conditions
0.8323	0.8438	0.7813	0.0923	0.0741	0.6889	0.6760	complex illumination
0.9000	0.9927	0.9197	0.1370	0.0735	0.7827	0.7803	cloud shadow affected

Issue: The method is sometimes hard to understand

We will add the following figure that will hopefully help readers no to get lost in section 4.2.3 between Fig. 6 & 7. The flow chart is in some aspect simplified (e.g. The mask is not mentioned since it is used in every single test). We will mention those simplifications in the caption.

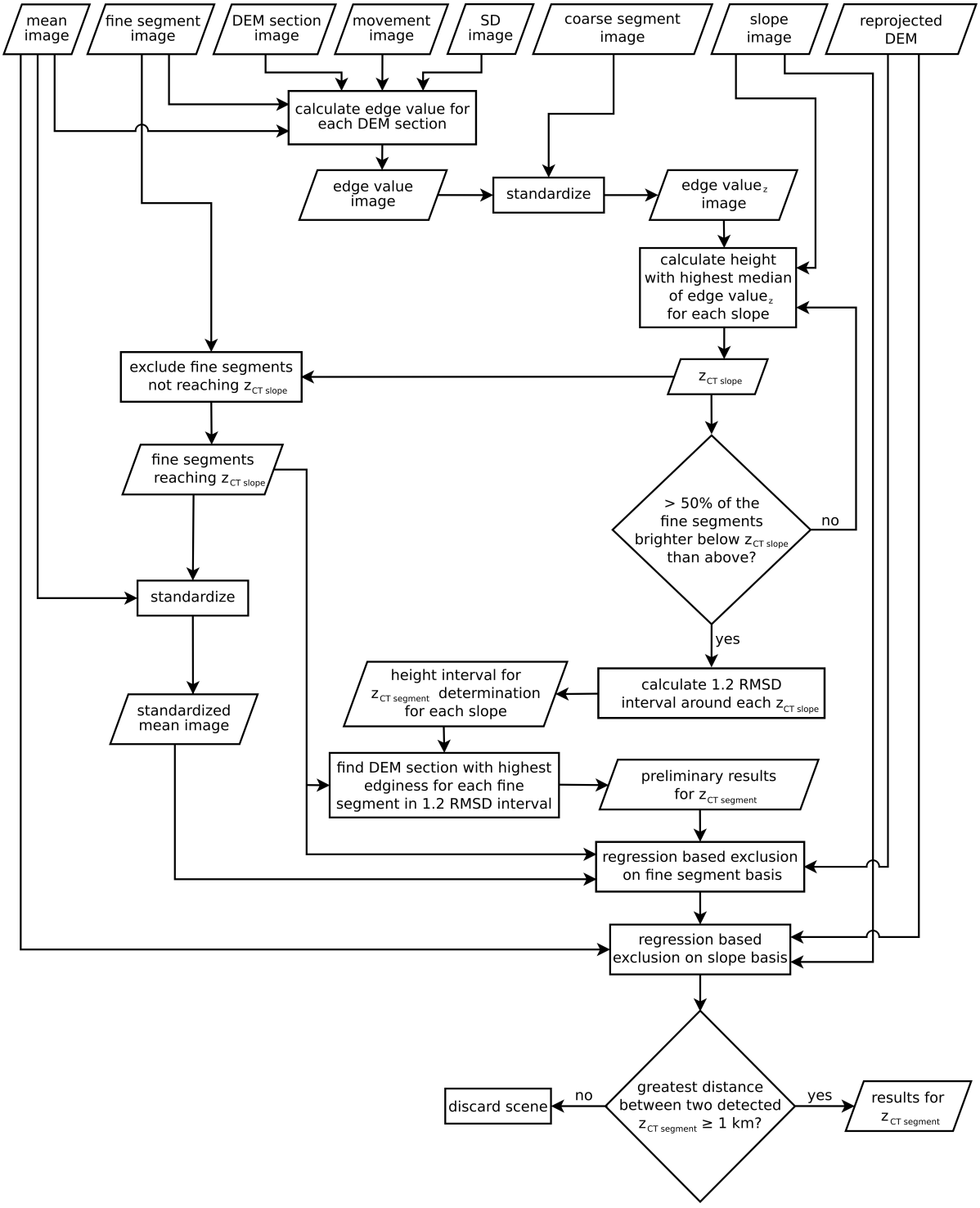

References

Cermak, J., Bendix, J. and Dobbermann, M.: FMet- an integrated framework for Meteosat data processing for operational scientific applications, Comput. Geosci., 34, 1638–1644, 2008.

Sæmundsson, T.: Atmospherice Refraction, Sky Telescope, 72, 70, 1986.

Tachikawa, T., Kaku, M., Iwasaki, A., Gesch, D., Oimoen, M., Zhang, Z., Danielson, J., Krieger, T., Curtis, B., Haase, J., Abrams, M., Crippen, R., and Carabajal, C.: ASTER Global Digital Elevation Model Version 2 – Summary of Validation Results. NASA Land Processes Distributed Active Archive Center and the Joint Japan-US ASTER Science Team, 2011.

Matthews, B. W.: Comparison of the predicted and observed secondary structure of T4 phage lysozyme, Biochim. Biophys. Acta, 405, 442–451, 1975.